Journal of Organometallic Chemistry 695 (2010) 1651–1656

Contents lists available at ScienceDirect

Journal of Organometallic Chemistry

journal homepage: www.elsevier.com/locate/jorganchem

Vibrational and DFT analysis of perfluoro-o-phenylenemercury compounds

Eliano Diana [a,*], Edoardo Marchese [b]

[a] Dipartimento di Chimica I.F.M, Università di Torino, Via Pietro Giuria 7, Torino 10125, Italy
[b] Dipartimento di Scienze e Tecnologie Avanzate, Università del Piemonte Orientale "A. Avogadro", Via T. Michel 11, Alessandria 15121, Italy

ARTICLE INFO

Article history:
Received 24 February 2010
Received in revised form
24 March 2010
Accepted 28 March 2010
Available online 21 April 2010

Keywords:
Perfluoro-o-phenylenemercury
DFT
Vibrational spectra

ABSTRACT

Vibrational spectra (infrared and Raman) for perfluoro-o-phenylenemercury and 1,2-bis(chloromercurio) tetrafluorobenzene were recorded for the first time. A DFT computation was performed and vibrational modes assigned. The effect of basis set of mercury was evaluated. This has permitted to obtain a "fingerprint" scheme of the $C_6F_4Hg_2$ unit, useful in the evaluation of intermolecular interaction of this family of compounds.

1. Introduction

Perfuorinated aromatic molecules play an important role in preparation of molecular material and in crystal engineering. This because their peculiar electrostatic properties, that favor quadrupolar interactions and the polarized C—F bonds that address directional intermolecular interactions. A significant molecule of this class is the $(C_6F_4Hg)_3$, perfluoro-o-phenylenemercury (**1**) compound [1], that combine the properties of fluorinated aromatic ring with a strong Lewis acidity[2,3]. This make this molecule able to form easily molecular complex with electron rich systems. His acidity comes from mercury atoms bonded to carbons made electron poor because the bond with fluorine atoms. CSD database reports 77 molecular complexes of **1**, and the most part possess face-to-face interactions with aromatic π-ring donor and C—F···H—C interactions. Usually infrared spectra of **1** [4] in his molecular complexes are reported, but a detailed vibrational analysis doesn't exist; for this reason no effect of coordinated guests onto vibrational spectra of **1** are reported, although vibrational spectroscopy is a very useful approach in evaluation of intermolecular interactions. A computational modeling of electronic spectra [5] report only a partial assignment of some modes. Considering the great interest for this compound we recorded complete vibrational spectra (infrared an Raman) and calculated DFT vibrational modes in order to propose an assignment. Complex **1** possess the idealized D_{3h} symmetry and may be resolved in three $C_6F_4Hg_2$ fragment of local C_{2v} symmetry. For this reason we analyzed also the $C_6F_4Hg_2Cl_2$, 1,2-bis(chloromercurio) tetrafluorobenzene (**2**) compound and compared his vibrational behavior with that of **1**.

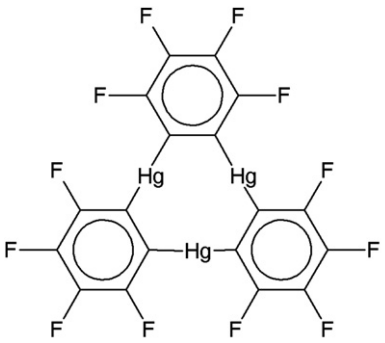

1 2

2. Experimental

Compound **1** was prepared following literature procedure [1,4]. Careful attention has devoted to purification because the existence of polymorphs. Four crystalline polymorph are reported for complex **1** [6]: two monoclinic with space group P21/n, one monoclinic with space group C2/c and one orthorhombic with

* Corresponding author. Tel.: +39 0 116707572; fax: +39 0 116707855.
E-mail addresses: eliano.diana@unito.it (E. Diana), edoardo.marchese@mfn.unipmn.it (E. Marchese).

0022-328X/$ – see front matter © 2010 Elsevier B.V. All rights reserved.
doi:10.1016/j.jorganchem.2010.03.031

space group Pnma. In this work we examined the P21/n form, that is the most common to obtain by crystallization from dichloromethane solution. We repeatedly crystallized the compound from dichloromethane, in order to obtain the P21/n form. Compound **2** was prepared by reaction of **1** with $HgCl_2$, according literature procedure [7]. Infrared spectra were recorded both in solid state and solution (CH_2Cl_2 and CS_2) spectra. We used KBr pellets for mid infrared and poliethylene for far infrared. Solid Raman spectra were recorded with grinded crystalline sample sealed in a glass capillary. FT-infrared and FT-Raman spectra were collected using the Bruker Vertex 70 FTIR spectrophotometer with the RAM II accessory, equipped with NdYAG laser (1064 nm) operated at 20–40 mW for solid and 200 mW for solution. Spectral resolution were 2 cm^{-1} for solid state and 4 cm^{-1} for solution spectra. Because the low solubility of compounds we cannot obtain useful solution Raman spectra. Low region of Raman spectra of powered samples were recorded with a Jobin Yvon-Horiba T64000 Raman Spectrometer, equipped with a confocal Olimpus Bx40 microscope; laser excitation was 752.5 nm with 500 mW starting power.

2.1. Details of DFT calculations

The quantum chemical calculations of compound **1** and **2** were carried out using the Gaussian09 code [8]. We used the DFT method using the hybrid three parameter B3LYP exchange-correlation and the ab initio MP2 method. The basis set employed are discussed in the result session. The structures are optimized to a real minimum (no imaginary frequencies) and analytical harmonic frequencies computed. Reported frequencies are scaled by a factor of 0.98.

3. Results and discussion

DFT modeling of organometallic compound is by now a common tool. Good performances are obtained with B3LYP hybrid functional and 6-31g(d,p)/LANL2DZ all electron/ECP mixed basis set, that allow at reasonable computing time to obtain good geometry and molecular properties, like vibrational and electronic spectra. With heavy elements nevertheless a great care is required because the significant relativistic effect that affects the evaluation of carbon-metal bond length [9]. For this reason Hg requires a basis set with a good representation of this effect. In Table 1 computed and experimental geometrical parameters for **1** and **2** compounds are reported. We have analyzed the effect of differing combinations of basis set for light elements and mercury in the geometry optimization of **2**. In DFT-a calculation we used the 6-31g(d,p) basis set for light elements and the common LANL2DZ basis set and pseudopotential for Hg. In the DFT-b computation we employed the very extended aug-cc-pvtz (C and F: 5s,4p,3d,2f; Hg: 6s,6p,5d,3f,2g)for all atoms, with a two component relativistic pseudopotential for inner shells of Hg [10]. In the DFT-c set we used 6-31g(d,p) basis set for light elements and aug-cc-pvtz with pseudopotential for Hg.

Table 1
Experimental and computed geometrical parameter of 1 and 2 molecules.

Bond length (Å) and angle	**2** exp. [19]	**2** DFT-a 6-31g (d,p) LANL2DZ	**2** DFT-b aug-CC-PVTZ aug-CC-PVTZ-PP	**2** DFT-c 6-31g(d, p) aug-CC-PVTZ-PP	**1** exp. [11]	**1** DFT-a 6-31g (d,p) LANL2DZ	**1** DFT-c 6-31g(d, p) aug-CC-PVTZ-PP
C–F	1.37(2)	1.343	1.338	1.342	1.350(14)	1.347	1.345
C–C	1.37(2)	1.393	1.389	1.395	1.382(17)	1.394	1.396
Hg–C	2.08(2)	2.203	2.078	2.072	2.066(12)	2.222	2.093
Hg–Cl	2.322(5)	2.420	2.302	2.304			
C–Hg–C					174.8(5)	170.01	174.43

Experimental data of **2** [19] show that C–C and C–F bonds have very similar length, also if the measurement's error is high. DFT calculation discriminate between these lengths, and basis set effect is very modest. Hg–C distance is more sensitive to basis set choice: the better representation of relativistic effect done by cc-pvtz basis set with pseudopotential gives a Hg–C bond distances very similar to that experimental. A good balance between time calculation and accuracy of results seems done by the DFT-c method. A similar behavior is found in **1**. The determination of C–F and C–C distances report a difference of nearly 0.05 Å, well reproduced by DFT calculation. Like in **2**, LANL2DZ doesn't reproduce well Hg–C distance and C–Hg–C angles, while the triple z basis set cc-pvtz-pp, gives values very near to those experimental.

These structural features are mirrored onto vibrational spectra. Compound **2** has a molecular symmetry represented by C_{2v} point group and 36 vibrational normal modes, that span the following irreducible representations and spectral activities:

$$I^{vib} = 11A_1(\mathrm{IR},\ \mathrm{Raman}) + 5A_2(\mathrm{Raman}) + 4B_1(\mathrm{IR},\ \mathrm{Raman}) + 10B_2(\mathrm{IR},\ \mathrm{Raman})$$

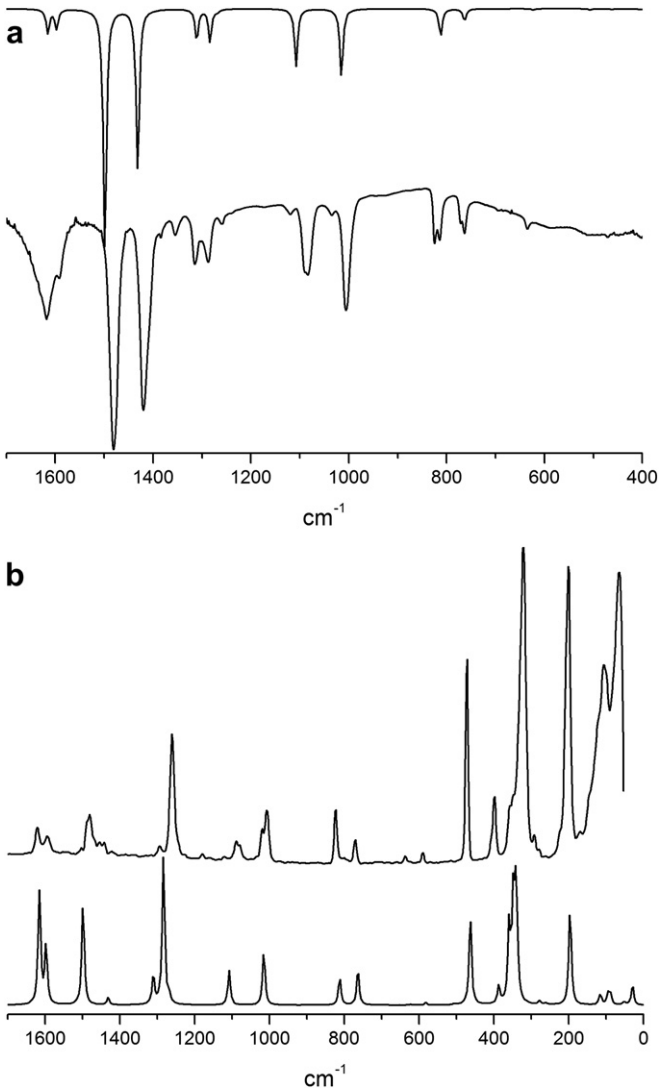

Fig. 1. (a) Infrared spectra of solid **2**. Experimental (bottom) and DFT-c (top). (**b**) Raman spectra of solid **2**: experimental (top) and DFT-c (bottom).

Table 2

2 DFT-a	**2** DFT-b	**2** DFT-c	**2** Infrared (solid)	**2** Raman (solid)		**1** DFT-c	**1** Infrared (solid)	**1** Infrared (CS_2 sol.)	**1** Raman (solid)		Assignment
1610	1597	1615	1621m	1621m	B_2	1616				A_2'	$\nu_{CC} + \alpha_{CCC}$
						1615	1617 m-w	1618 m-w	1617s	E′	
1597	1564	1597	1593m	1593 m-w	A_1	1593				A_1'	$\nu_{CC} + \nu_{CF}$
						1589	1585 w	1584 w	1585m	E′	
1494	1475	1483	1481 vvs	1481s	A_1	1496			1491 m-w	A_1'	ν_{CF}
						1487	1474 vs	1475 vs	1477 w	E′	
1424	1411	1433	1420 vs	1420vw	B_2	1429	1426 sh, 1419s		1419 w	E′	$\nu_{CC} + \nu_{CF}$
						1416				A_2'	
1303	1293	1311	1314m		A_1	1312			1309 w, sh	A_1'	ν_{CC}
						1310	1309m	1306 m-w		E′	
1281	1261	1284	1288m	1293 w	A_1	1271			1295 w	A_1'	$\nu_{CC} + \nu_{CF} + \nu_{Hg-C}$
						1269	1291m	1289m-s	1289 m-w, sh	E′	
1259	1242	1268	1260 w	1260 vs	B_2	1262				A_2'	$\nu_{CC} + \alpha_{CCC} + \nu_{Hg-C}$
						1259	1256m	1254m	1256s	E′	
1100	1086	1107	1088, 1082 m	1088, 1082m	A_1	1101	1090m	1087s		E′	$\nu_{CF} + \alpha_{CCC} + \nu_{Hg-C}$
						1101			1093 m-w	A_1'	
999	1007	1015	1006s	1006s	B_2	1011	1009s	1009 vs	1016m, br	E′	$\nu_{CC} + \alpha_{CCC} + \nu_{Hg-C}$
						1011				A_2'	
778	811	812	824, 814m	824s	B_2	814				A_2'	$\nu_{CC} + \alpha_{CCC} + \nu_{Hg-C}$
						804	819m	817s	819 w	E′	
736	758	763	770, 764m	770m	A_1	764	774 w			E′	$\nu_{CC} + \nu_{CF} + \alpha_{CCC} + \nu_{Hg-C}$
						762			774s	A_1'	
677	693	688	695 vw		B_2	689			700m	E′	$\alpha_{FCC} + \alpha_{HgCC}$
						667				A_2'	
653	747	651			A_2	657			638 m-w	E″	γ_{CCC}
						651				A_1''	
622	650	623	636 w	636 w	B_1	625				A_2''	γ_{CCC}
						620			617 vw, br	E″	
566	605	582		591 w	A_2	585			600m	E″	γ_{CCC}
						572				A_1''	
502	511	507			B_2	505				A_2'	$\alpha_{CCC} + \nu_{Hg-C} + \nu_{Hg-x}$
						504				E′	
458	464	464	471 vw	472 vvs	A_1	463	472 w			E′	$\alpha_{CCC} + \nu_{Hg-C} + \nu_{FC}$
						462			472 vs	A_1'	
384	393	387		398s	A_2	395			414s	E″	$\gamma_{FCC} + \gamma_{CCC}$
						382				A_1''	
314	342	360	334 vs	334 vs (sh)	A_1						ν_{Hg-Cl}
310	347	349	315vs	322 vvvs	B_2						ν_{Hg-Cl}
337	348	346	358m	358s, sh	B_1	361	372m			A_2''	$\gamma_{FCC} + \gamma_{CCC}$
						330			353 vs	E″	
343	358	341	349m	348s, sh	A_1	345	336 w			E′	$\delta_{CFC} + \nu_{Hg-C}$
						343			340s, sh	A_1'	
276	286	278	277 w (sh)	278 w, sh	B_2	276	289 m-w		289 vw	E′	δ_{CFC}
						276				A_2'	
261	273	262		262 vw	A_1	261	278 w		278 w	E′	δ_{CFC}
						261				A_1'	
179	200	197	210s	210 w (sh)	B_1	213				A_2''	γ_{FCC}
						180				E″	
172	196	197	200, 193s	200s	A_1	219	222m		225 w	E′	ν_{Hg-C}
						177			186 vvs	A_1'	
165	195	196	200, 193s	199m (sh)	B_2	186				A_2'	ν_{Hg-C}
						183			186 vvs	E′	
157	159	157	155 (vvw)		A_2	155			154 vw	E″	γ_{CCC}
						154				A_1''	
107	113	114		122m-s	B_1	114	120 w, br			A_2''	γ_{CCC}
						105			120 vw	E″	
98	117	117			B_2	104				A_2'	$\alpha_{CCHg} + \nu_{Hg-C} + \nu_{Hg\cdots Hg}$
						97	101 vw		101 vs	E′	
74	95	95	94s	95m-s	A_1						δ_{ClHgC}
						94	96 vw		96m	A_1'	$\nu_{Hg\cdots Hg}$
72	87	88			A_2	62			63s	E″	ring tors.
44	55	55			B_2	40	45 m-w		45 vs	E′	ring i.p. bend.
46	51	52	52m sh	53s	B_1	22				A_2''	ring o.o.p. bend.
36	35	37			A_2	38				A_1''	ring tors.
						17			17m	E″	
27	30	29		29 vs	A_1						α_{ClHgC}

In Fig. 1 a and b solid state experimental and DFT-c infrared and Raman spectra are reported. The 100 cm^{-1} region of experimental Raman is not significative because very close to the cut of Rayleigh filter of the FT-Raman instrument employed. Compound **2** belong to P21/n space groups, with $Z = 8$ and a double occupancy of general position [19]. For this reason we expect doubling of spectral features, with the same intensities. Comparison of experimental and DFT pattern shows that solid state may be easily traced back to molecular spectra. In Table 2 we reported the one-to-one correspondence of fundamental normal modes, with their assignment obtained by analysis of internal coordinate composition.

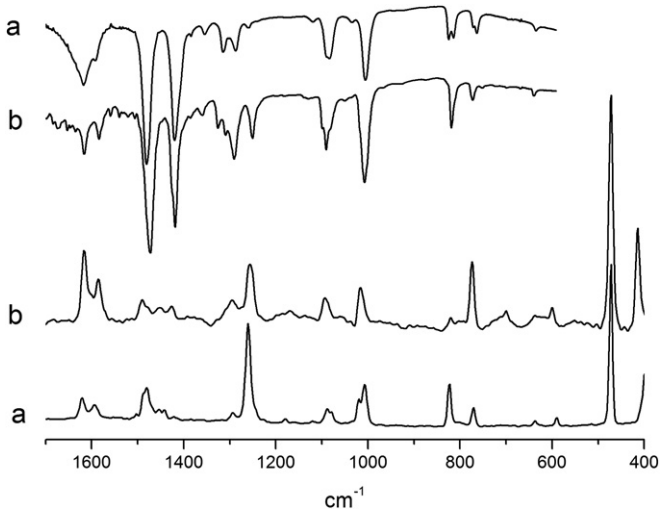

Fig. 2. Infrared (top) and Raman (bottom) spectra of compound **2** (**a**) and **1** (**b**) in solid state.

We reported DFT results obtained with the three basis set combinations discussed upon: the mean differences between DFT and experimental frequencies are respectively 17.4, 11.5 and 8.4 cm^{-1}, and this confirm that the 6-31g(d,p)/cc-pvtz-pp mixed basis set reproduces accurately the experimental frequencies. Infrared intensities are in good accord with experimental data, while computed intensities of Raman spectrum is not equally accurate for all vibrational modes (Fig. 1b); this is justifiable by the difficulty of DFT methods to reproduce satisfactorily the polarization changes of molecules, especially when large and very polarizable atoms like Hg are involved. Nevertheless the pattern is comparable with that experimental. Similarly to the assignments proposed for hexafluorobenzene [12,13] and 1,2-diiodotetrafluorobenzene [14] we may distinguish two spectral regions: one comprise between 1600 and 700 cm^{-1}, characterized mainly by bond's stretching and planar angular modes of C_6F_4 unit, and one comprise between 700 and 30 cm^{-1}, where are the out-of-plane deformation modes and the modes involving mainly the mercury atoms. We discuss these two regions separately.

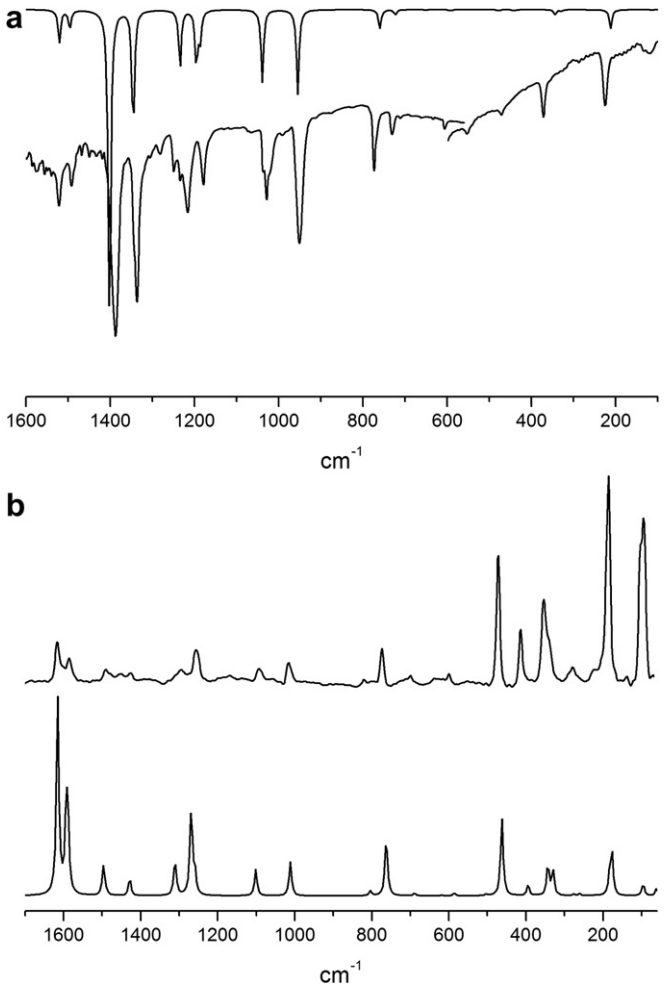

Fig. 3. (**a**): Infrared spectra of solid **1** : DFT-c (top) and experimental (bottom). (**b**): Raman spectra of solid **1** : DFT-c (bottom) and experimental (top).

Table 3
correlation table between C_{2v} and D_{3h} point group.

C_{2v}	→	D_{3h}
A_1	→	A_1'
B_2	→	A_2'
$A_1 + B_2$	→	E'
A_2	→	A_1''
B_1	→	A_2''
$A_2 + B_1$	→	E''

1600–700 cm^{-1} region

In this region are the most intense infrared bands, and the most important modes are the C–C and C–F stretching. Because the similar atomic mass and bond length, the composition of normal modes shows a strong mixing of ν(CC) and ν(CF), with a significant involvement of Hg–C stretching and C–C–C angle bending. All infrared features are broad and the modes at 1088, 824 and 770 cm^{-1} are split because of factor group effect. The very strong 1481 cm^{-1} mode is the total symmetric ν(C–F) stretching and the 770 cm^{-1} mode corresponds to the ring breathing of benzene molecule. Normal modes between 1260 and 770 cm^{-1} have a significant component of Hg–C stretching, and for this reason may be sensible to change of electronic properties of mercury atom.

700–50 cm^{-1}

Raman spectrum has very intense bands in this region, where fall the in-plane and out-of-plane C–F and C–C–C deformation modes and the C–Hg stretching and bending modes. Also these mode are strongly mixed because the great mass of mercury atoms. In benzenoid systems the all-in-phase C–H bending, both in plane and out-of-plane, are usually very sensitive to intermolecular interactions [15]; in compound **2** the corresponding δ(CFC) and γ (FCC), are at 695 and 210 cm^{-1}. DFT calculations with all the three basis set choices report that ν(HgCl) modes have a coupling of 5–10 cm^{-1}; **2** has the two ν(HgCl) Raman modes at 383(w) and 314 (vs) cm^{-1}. We assign one mode to the strong Raman at 322 cm^{-1} and the other to the strong infrared at ca 334 cm^{-1}. The 472 cm^{-1} strong band is assigned to the C–C–C angle deformation, corresponding to prolate ellipse deformation of C_6F_4 ring. The two uncoupled ν(HgC) modes are assigned to the strong band at 200 cm^{-1}. Low Raman region (80–5 cm^{-1}) shows many features, attributable both to intramolecular vibrational modes and to molecular librational and translational modes. On the basis of intensity comparison between DFT and experimental data we assign the strong 95 cm^{-1} band to the in-plane Cl–Hg–C bending; the 53 cm^{-1} band to the out-of-plane bending of the C_6F_4 ring and the very strong feature at 29 cm^{-1} to the Cl–Hg–C scissoring mode.

Analysis of vibrational spectra of **1** was performed by comparison of the spectra of compound **1** and **2**. Fig. 2 shows vibrational spectra (in mid-infrared region) of **1** compared with **2**.

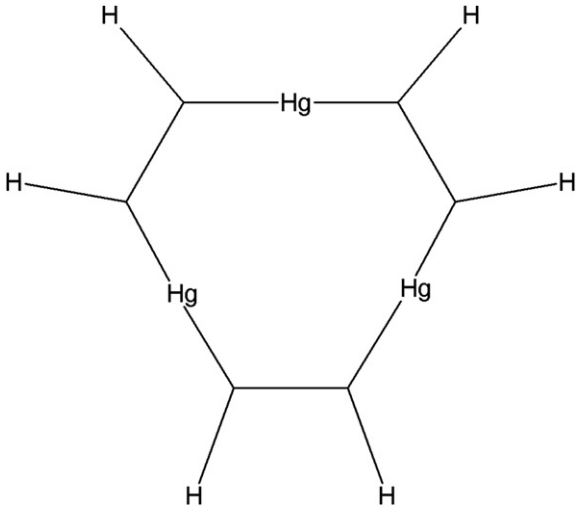

Fig. 4. Scheme of the simplified $(C_2H_2Hg)3$ model used to evaluate the Hg…Hg vibrational modes.

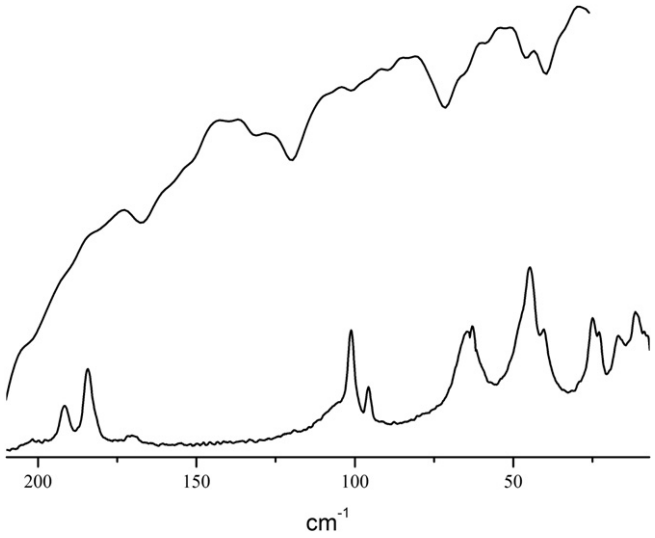

Fig. 5. Infrared (top) and Raman (bottom) spectra of compound **1** in the low frequency region (solid state).

It's evident the strict similarity between the pattern of the two compounds. This suggests that vibrational analysis of compound **1** may be carried out by considering the complex composed of three uncoupled C_6F_4 units bound to a Hg_3 triangle. DFT-c calculations confirm this statement.

Compound **1** has 93 vibrational normal modes, that in D_{3h} point group symmetry span the following irreducible representation:

$$\Gamma^{vib} = 11A_1'(\text{Raman}) + 10A_2'(\text{n.a.}) + 21E'(\text{IR, Raman}) + 5A_1''(\text{n.a.}) + 5A_2''(IR) + 10E''(\text{Raman})$$

The molecule plane is oriented in the xy plane and z coincide with molecular C_3 axis: for consequence planar modes are assigned to A_1', A_2' and E' species, while out-of-plane normal modes are assigned to A_2'' and E'' species. In Table 2 calculated vibrational frequencies are reported with the assignment obtained by analysis of normal mode in term of internal coordinates. Comparison of computed vibrational frequencies and intensities with experimental infrared and Raman data has permitted the assignment of fundamental modes. The one-to-one correspondence is generally satisfactory (Fig. 3a and b).

In the table normal modes of **2** are correlated with those of **1** through the correlation table between the molecular point groups C_{2v} and D_{3h} (Table 3):

In Table 2 normal modes of **1** are reported in correspondence of those of **2**. A comparison of experimental solid state and solution infrared spectra with DFT results shows that solid state spectra is very similar to that molecular. This indicates that factor group splitting or solid state effects don't affect strongly the vibrational pattern for this molecules, similarly to compound **2**. Any mode of C_6F_4 unit in **2** has a corresponding A type and doubly degenerate E type mode in **1**. DFT and experimental data show that the A and E modes of **1** derived from corresponding modes of **2** have very similar frequencies, with a separation of 5–10 cm^{-1}. This indicate that the coupling between the three C_6F_4 units is negligible and consequently that through-space dipolar interaction between C–F bonds is very weak. This may explicate why also factor group splitting is of modest entity and why only strong intermolecular interaction may have effect onto vibrational spectra.

The six ν(HgC) modes are computed at 219 (E′), 177 (A_1'), 186 (A_2') and 183 (E′) cm^{-1}; the coupling between the two E′ modes is 36 cm^{-1} and the barycentre is at 201 cm^{-1}, very similar to the uncoupled ν(HgC) at 200 cm^{-1} of compound **2**. Consequently we assigned ν(HgC) to the medium infrared band at 222 cm^{-1} and to the strong Raman band at 186 cm^{-1}.

The most interesting feature of the compound **1** is the Hg_3 core, where the proximity of mercury (II) centers (3.62 Å) produce Hg···H interactions and is responsible of the remarkable Lewis acidity of **1** [5]. Vibrational detection of metallophilic interactions is not commonly reported. For the adducts involving $Ag(CN)_2^-$ and $Au(CN)_2^-$ systems the metallophilic Ag···Au interaction is indirectly detected from the influence onto the metal-carbon stretching mode [16]. An ab initio study of the $HgMe_2$ dimer [17] report for a 'T' shaped structure a Hg–Hg distance of 3.408 Å and a Hg···Hg frequency of 33 cm^{-1}. In complex **1** analysis of DFT results shows three normal modes attributable to the Hg_3 skeleton: a double degenerate E′ mode at 97 cm^{-1} and a A1′ mode at 94 cm^{-1}. A guess to the normal mode composition shows that these modes involve also the Hg–C bonds. In order to evaluate the effect of the contribution from the C_6F_4 ring onto these modes we performed a vibrational analysis of a simplified $(C_2H_2Hg)_3$ system (Fig. 4)

This system has the same D_{3h} symmetry of **1** and contains the same $(C_2Hg)_3$ framework. Theoretical evaluation of metallophilic interaction must consider accurately electronic correlation effects and take in account dispersion interactions [5,17,18]. For this reason we optimized and calculated vibrational modes for the $(C_2H_2Hg)_3$ system with the DFT-c method and at MP2 level. In Table 4 we report the most relevant results.

DFT-c computed Hg–Hg and Hg–C distances for **1** are respectively 3.683 and 2.093 Å, comparable to that of $(C_2H_2Hg)_3$ system, while the MP2 values of $(C_2H_2Hg)_3$ are comparable to the experimental values of **1**. Clearly the dispersion contribution influence the geometrical parameter of Hg_3 ring, but, interestingly, the vibrational stretching modes don't seem influenced. If we compare the DFT-c values with the corresponding vibrational modes of complex **1** we can observe that the A1′ mode has a similar frequency and that the three $\nu_{Hg\cdots Hg}$ modes are almost uncoupled, whereas the E′ mode of $(C_2H_2Hg)_3$ is lower of nearly 40 cm^{-1}. An examination of

Table 4
geometrical and vibrational parameter of $(C_2H_2Hg)_3$.

	$d_{Hg\text{-}Hg}$(Å)	d_{C-Hg}	$\nu_{Hg\cdots Hg}$ (E′)	$\nu_{Hg\cdots Hg}$ (A_1')
DFT-c	3.630	2.095	58	97
MP2	3.481	2.037	56	103

the A1′ mode in both the systems shows that is mainly a breathing mode of the Hg_3 triangle, mixed with the C–C–Hg angle's bendings; the E′ modes, apart the Hg···Hg stretching, involve the shifting of all the C_2H_2 or C_6F_4 units, and for this reason the mass difference of these fragments can justify the frequency difference.

A comparison of the computed frequencies with the experimental data in the low frequency region and considering the intensity pattern expected for the D_{3h} selection rules (Fig. 5), permit us to assign the Hg···Hg stretching modes to the two Raman features 101 cm^{-1} (E′) and 96 cm^{-1}.(A_1′).

Vibrational assignment of **2** is in accord with the assignment proposed for 1,2-diiototetrafluorobenzene [14]: the six strongest infrared features for this molecule are found at 1491, 1442, 1111, 1028, 819 and 777 cm^{-1}. The pattern is the same of **1** and **2**, with a shift to higher frequencies that may be attributed to the different mass effect of iodine and mercury in the mixed modes of this region.

4. Conclusions

The comparison between the vibrational spectra of two perfluorinated phenylenemercury compound shows that C_6F_4 unit presents a reproducible pattern, with very poor solid state effects. DFT modeling with B3LYP hybrid functional and 6-31g(d,p) (C, F)/cc-pvtz-pp (Hg) basis set permit a good reproduction of structural parameter and an accurate calculation of vibrational frequencies and infrared intensities. This has permitted to assign the fundamental modes of vibrational spectra of $C_6F_4Hg_2Cl_2$ and of $(C_6F_4Hg)_3$ compound and to trace a "fingerprint" pattern for the $C_6F_4Hg_2$ fragment, useful in the evaluation of intermolecular interactions, that are of great importance in the molecular engineering where this kind of systems are commonly employed. Analysis of the low frequency region permits to assign the Hg···Hg modes, usually involved in a metallophilic interactions.

References

[1] P. Sartory, A. Golloch, Chem. Ber. 101 (1968) 2004.
[2] M.R. Haneline, R.E. Taylor, F.P. Gabbaï, Chem. Eur. J. 9 (2003) 5188–5193.
[3] R.J. Taylor, C.N. Burress, F.P. Gabbaï, Organometallics 26 (2007) 5252–5263.
[4] A.S. Filatov, E.A. Jackson, L.T. Scott, M.A. Petrukhina, Angew. Chem. Int. Ed. 48 (2009) 8473.
[5] A. Muñoz-Castro, D. MacLeod Carey, R. Arratia-Pérez, J. Phys. Chem. A 114 (2010) 666.
[6] M.R. Haneline, F.P. Gabbaï, Z. Naturforsch. B 59 (2004) 1483.
[7] A.G. Massey, N.A.A. Al-Jabar, R.E. Humphries, G.B. Deacon, J. Organomet. Chem. 316 (1986) 25.
[8] M.J. Frisch, G.W. Trucks, H.B. Schlegel, G.E. Scuseria, M.A. Robb, J. R. Cheeseman, G. Scalmani, V. Barone, B. Mennucci, G.A. Petersson, H. Nakatsuji, M. Caricato, X. Li, H.P. Hratchian, A.F. Izmaylov, J. Bloino, G. Zheng, J.L. Sonnenberg, M. Hada, M. Ehara, K. Toyota, R. Fukuda, J. Hasegawa, M. Ishida, T. Nakajima, Y. Honda, O. Kitao, H. Nakai, T. Vreven, J. A. Montgomery Jr., J.E. Peralta, F. Ogliaro, M. Bearpark, J.J. Heyd, E. Brothers, K. N. Kudin, V.N. Staroverov, R. Kobayashi, J. Normand, K. Raghavachari, A. Rendell, J.C. Burant, S.S. Iyengar, J. Tomasi, M. Cossi, N. Rega, J.M. Millam, M. Klene, J.E. Knox, J.B. Cross, V. Bakken, C. Adamo, J. Jaramillo, R. Gomperts, R. E. Stratmann, O. Yazyev, A.J. Austin, R. Cammi, C. Pomelli, J.W. Ochterski, R. L. Martin, K. Morokuma, V.G. Zakrzewski, G.A. Voth, P. Salvador, J. J. Dannenberg, S. Dapprich, A.D. Daniels, Ö Farkas, J.B. Foresman, J.V. Ortiz, J. Cioslowski, D.J. Fox, Gaussian 09, Revision A.02. Gaussian, Inc., Wallingford CT, 2009.
[9] P. Pyykkö, Chem. Rev. (1988) 563.
[10] K.A. Peterson, C. Puzzarini, Theor. Chem. Acc. 114 (2005) 283.
[11] M.R. Haneline, M. Tsunoda, F.P. Gabbaï, J. Am. Chem. Soc. 124 (2002) 3737.
[12] D. Steele, D.H. Whiffen, Trans. Faraday Soc. 55 (1959) 369.
[13] D.A. Braden, B.S. Hudson, J. Phys. Chem. A 104 (2000) 982.
[14] R.A. Yadav, I.S. Singh, O. Sala, J. Raman Spectr. 14 (1983) 353.
[15] P.L. Stanghellini, E. Diana, A. Arrais, A. Rossin, S.F.A. Kettle, Organometallics 25 (11) (2006) 5024.
[16] J.C.F. Colis, R. Staples, C. Tripp, D. Labrecque, H. Patterson, J. Phys. Chem. B 109 (2005) 102–209.
[17] P. Pyykkö, M. Straka, Phys. Chem. Chem. Phys. 2 (2000) 2489–2493.
[18] F. Mendizabal, D. Burgos, C. Olea-Azar, Chem. Phys. Lett. 463 (2008) 272–277.
[19] J.D. Beckwith, M. Tschinkl, A. Picot, M. Tsunoda, R. Bachman, F.P. Gabbaï, Organometallics 20 (2001) 3169.

Eliano Diana was born in Turin in 1965; PhD in chemistry in 1994, faculty researcher in 1992 and associate professor in general and inorganic chemistry in 2007 at the university of Turin. His main research interests are in vibrational study and DFT modeling of organometallic complexes.

Edoardo Marchese was born in Turin in 1983; PhD in chemistry in 2008 at university of Turin. Now is postdoctoral fellow at university of Eastern Piedmont. His main research interest are in the synthesis and characterization of molecular complexes of organometallic compound.